## IV.9. IRON FISCHER-TROPSCH CATALYST. PREPARATION OF $\gamma$-FEOOH FORM FERRIC SALT SOLUTIONS (Sivaraj Chokkaram, Diane R. Milburn and Burtron H. Davis)

### IV.9.1. ABSTRACT

Ferric iron (ferrihydrite) was precipitated from ferric salt solutions, and this was then transformed to produce crystalline FeOOH. Hydrazine was used as the transformation agent. Several factors, such as pH, counter ions, nature and amount of the chemical modifier affect the ferrihydrite transformation process. The results of the present study identify the role of hydrazine and chloride ions during the transformation of ferrihydrite to $\gamma$-FeOOH.

### IV.9.2. INTRODUCTION

Iron hydroxides, oxyhydroxides and oxides are used extensively as pigments, catalysts, co-catalysts, flocculents etc. Furthermore, corrosion of iron or steel results in the formation of rust, which consists of one or more iron hydroxides or oxyhydroxides and oxides. Despite numerous studies about the synthesis of iron hydroxides/oxyhydroxides, much is not known about the mechanism of the formation of these products. For example, the oxidation products of aqueous $Fe(OH)_2$ may be $\alpha$-FeOOH, $\gamma$-FeOOH or $\delta$-FeOOH, depending on the experimental conditions such as nature of oxidizing agent, pH, oxidation temperature, $Fe^{2+}$ concentration, etc. Moreover, the formation of these products proceeds through an intermediate iron complex, commonly known as 'green rust'. The exact structure and composition of this intermediate compound is not known. However, it is possible to predict the final oxidation products if the experimental conditions are known.

Hydrolysis and precipitation studies of iron solutions have attracted attention for a long time. Dousma and Bruyn (IV.9.1-IV.9.3) studied extensively the hydrolysis and precipitation of aqueous ferric nitrate solutions. Matijevic and Janauer (IV.9.4) reviewed various aspects on the hydrolysis of iron(III) ions in aqueous media. Flynn (IV.9.5) reviewed various aspects of the hydrolysis reactions involving ferric ions in aqueous media, including aqueous Fe(III) species, formation of polymeric products and their composition, aging of the polymeric products, and the nature of the aged products under various conditions. The precipitation and/or hydrolysis products of ferric nitrate or chloride aqueous solutions may be $\alpha$-FeOOH, $\beta$-FeOOH, or amorphous iron hydroxide/oxyhydroxides, depending on the pH of precipitation, temperature, aging and other experimental variables. When ferric hydroxide is precipitated at room temperatures and high pH values (>11.00) the resulting precipitate is often $\alpha$-FeOOH, whereas at pH values <10.00 the final product is usually amorphous.

Possible structural transformations among iron hydroxides and oxides have been reported by Bernal et. al (IV.9.6). Although the transformation of amorphous ferric hydroxide to $\alpha$-FeOOH has been studied widely, those of the transformation of amorphous ferric hydroxides to $\gamma$-FeOOH are quite limited. Usually $\delta$-FeOOH is prepared by oxidation of $Fe(OH)_2$ aqueous suspensions. In this paper, we report a direct synthetic route for the preparation of pure $\gamma$-FeOOH from either ferric nitrate or ferric chloride aqueous solutions. The scope of the present study is to define the effect of pH, iron precursor, and nature of the chemical modifier on the crystallinity, BET surface area, and pore volume of the product.

## IV.9.3. EXPERIMENTAL

### IV.9.3.a. Chemicals

Ferric chloride (analytical grade, Mallinckrodt), ferric nitrate (analytical grade, Johnson Matthey), hydrazine monohydrate (analytical grade, Aldrich), sodium hydroxide (analytical grade, Aldrich), pyridine (analytical, Aldrich), ethyl Pyridine (analytical grade, Aldrich), and ammonium chloride (analytical grade, Aldrich) were used.

### IV.9.3.b. Preparation

#### IV.9.3.b.1. From Ferric Chloride

Ferric hydroxide was precipitated from an aqueous solution of ferric chloride in three series of experiments. In the first, iron(III) hydroxide was precipitated by adding aqueous NaOH solution (5M) to a ferric chloride aqueous solution (0.5M, and 500 ml) to produce a final pH value ranging from 5 to 10. The precipitation was performed at room temperature. The iron(III) hydroxide/ or oxyhydroxide was collected by filtration, washed thoroughly by repeated slurrying with distilled water, and then dried at 900°C for 20 hr.

The second series of experiments was the same as the first series except the precipitate was treated with 0.0618 moles of hydrazine prior to filtration, washing, and drying. In the third series of experiments iron(III) hydroxide was precipitated at a pH of about 6.3 and this was followed by the addition of different amounts of hydrazine ranging from 0.005 to 0.0618 moles prior to filtration and drying. In the later two series of experiments, the precipitates were stirred for 30 minutes after adding the hydrazine and prior to the filtration step.

IV.9.3.b.2. From Ferric Nitrate

(1) Ferric hydroxide was precipitated by adding the aqueous NaOH solution (5M) to a 0.5 M solution of iron (III) nitrate to produce pH values ranging from 5 to 10. The resulting precipitate was collected by filtration, washed, and dried at 900°C for 20 hr.

(2) Ferric hydroxide was precipitated with aqueous NaOH (5M) and the resulting precipitate was divided into two portions. One portion was treated with hydrazine and equilibrated for 30 minutes prior to filtration, washing and drying. The second portion was collected by filtration, washed and reslurried in 500 ml of 0.5 M ammonium chloride solution; this was followed by a treatment with hydrazine prior to filtration, washing, and drying.

(3) Ferric hydroxide was precipitated from a ferric nitrate aqueous solution (0.5M) with aqueous sodium hydroxide solution (5M) at pH values ranging from 5 to 9. The resulting precipitates were collected by filtration, reslurried in 500ml of 0.5M $NH_4Cl$ aqueous solution, equilibrated for 30 minutes, and then treated with 0.0618 moles of hydrazine. The precipitates were equilibrated for another 30 minutes prior to filtration, washing and drying.

(4) Ferric hydroxide was precipitated from a ferric nitrate aqueous solution (0.5M) with aqueous sodium hydroxide (5M) at a pH of about 6.3. The resulting precipitate was then reslurried in 500ml of 0.5M $NH_4Cl$ equilibrated for 30 minutes, and then treated with different amounts of hydrazine ranging from 0.005 to 0.0618 moles. The precipitates were equilibrated for another 30 minutes prior to filtration, washing and drying.

IV.9.3.b.3. Effect of Other Chemical Modifiers

In a typical experiment ferric hydroxide was precipitated from ferric chloride solution (0.5M) with aqueous sodium hydroxide (5M) at a pH value of 6.3. The resulting precipitate was treated with pyridine (about 0.10 moles), then equilibrated for 30 minutes, followed by filtration, washing, and drying at 90°C. Similar type of experiments were performed using ethylpyridine, and hydrazine carboxylate instead of pyridine.

IV.9.3.b.4. BET Surface Areas and Pore Size Distribution

Nitrogen sorption isotherms were measured using a Quantachrome Autosorb 6 instrument following outgassing the samples at 80°C and < 5 mtorr for at least 8 hours. Surface areas were calculated using the BET equation (IV.9.7) and the nitrogen sorption data. Pore size distributions were calculated from the desorption data assuming a cylindrical pore shape with refinements developed by Broekhoff and deBoer (IV.9.8) which correct for a stable adsorbed layer of nitrogen. This model was chosen over packed particle models and other cylindrical pore models because it provides better agreement with the BET surface area and Gurvitsch pore volume.

IV.9.3.b.4. X-Ray Diffraction Measurements

X-ray diffraction measurements were accomplished using a Philips X-ray diffractometer at 25kv, 20 mA and CuK$\alpha$ radiation ($\lambda$ = 1.5418A). The identification of the phases in the products was accomplished by comparing the standard ASTM diffraction pattern of the expected compound to the sample. The diffraction peaks which match are marked accordingly. This process was repeated with several expected iron compounds which enabled an identification of the various phases in the sample.

## IV.9.4. RESULTS AND DISCUSSION

The effect of the final pH, and hydrazine on the BET surface area, pore volume and crystal structure of ferric iron precipitated from ferric chloride aqueous solutions are summarized in Table IV.9.1. XRD patterns (Figure IV.9.1) show that the samples are amorphous, except for the sample precipitated at pH= 9.93 and even this sample is poorly crystalline material exhibiting few diffraction lines. These peaks obtained for the sample precipitated at pH = 9.93 could not be matched with any hydroxides or oxyhydroxides of iron. The XRD patterns of ferric hydroxides, precipitated at pH values ranging from 5.00 to 9.30 from ferric chloride aqueous solutions, that were subjected to the chemical treatment with hydrazine following precipitation but prior to filtration show (Table IV.9.1 and Figure IV.9.2) that all of the materials are crystalline. Thus, the addition of hydrazine has either induced or accelerated the crystallization process. The results show that at pH values less than about 8.00 the final product is mostly $\gamma$-FeOOH (lepidocrocite), while at pH values greater than 9.00 the products are predominantly $\alpha$-FeOOH (goethite) with small amounts of $\gamma$-FeOOH.

The data in Table IV.9.2 summarizes the effect of hydrazine on the BET surface area, pore volume, and crystal structure of iron hydroxides /or oxyhydroxides precipitated from ferric chloride at a constant pH ($\sim$6.30) followed by treatment with different amounts of hydrazine. The XRD results (Figure IV.9.3) results show that the crystallinity of the material depend on the amount of hydrazine added, with the crystallinity of FeOOH increasing with increasing hydrazine concentration to attain a maximum after which further increases in hydrazine concentration causes a decrease in the crystallinity. Even at low concentrations of hydrazine, the product is mostly $\gamma$-FeOOH with only a small amount of

$\alpha$-FeOOH. As the hydrazine concentration is increased the amount of $\alpha$-FeOOH also increase. An explanation for could involve the formation of an iron-hydrazine complex that upon decomposition leads to crystalline FeOOH. The final pH of the suspension depends upon the amount of hydrazine added, and increases with increasing hydrazine concentration. The crystal structure that forms may be governed by the pH of the suspension following hydrazine addition. The XRD results (Figure IV.9.4) for the iron hydroxides precipitated from ferric nitrate solutions at pH values ranging from 5.00 to 10.00 show only amorphous phases are present up to a pH of 9. The peak at $2\theta = 44$ should be ignored since it is caused by the instrument. Again the material precipitated at a pH of 10 does have some crystallinity. The XRD patterns of all of the samples, precipitated from ferric nitrate aqueous solutions followed by chemical treatment with, ammonium chloride and hydrazine monohydrate prior to filtration show the presence of iron oxyhydroxide phases (Figure IV.9.5). The material precipitated directly from ferric nitrate followed by chemical treatment with hydrazine produce a mixture of $\alpha$ and $\gamma$-FeOOH. On the other hand, when a portion of the sample is filtered, treated with ammonium chloride followed by treatment with hydrazine, it produced $\gamma$-FeOOH with only traces of $\gamma$-FeOOH. Under the experimental conditions employed, these results make it clear that the chloride ion is involved along with hydrazine in determining the crystal structure of FeOOH. The data in Tables IV.9.3 and IV.9.4 summarize the results of the effect of precipitation pH and hydrazine on the crystal structure, BET surface area, and pore volume of FeOOH precipitated from ferric aqueous solution followed by filtration, reslurrying in ammonium chloride, and treatment with hydrazine prior to final filtration, washings, and drying. The XRD patterns (Figure IV.9.6) show that the crystal structure

is very much dependent on the precipitation pH at the end of the precipitation step (i.e. pH1). $\gamma$-FeOOH is present for values of pH although but the relative intensity amount of $\gamma$-FeOOH varies with pH. The amount of $\gamma$-FeOOH phase increases with an increase of pH up to $pH_1 = 7$ but with a further increase in $pH_1$ above 7.00 the relative amount of $\gamma$-FeOOH decreases. Thus, the relative amount of the $\alpha$-FeOOH phase increases with an increase of $pH_1$. The results clearly show the formation of crystalline FeOOH when the material is precipitated from ferric nitrate followed by treatment with ammonium chloride and hydrazine. However, the relative amounts of $\alpha$ and $\gamma$-FeOOH is controlled by the precipitation pH (i.e $pH_1$) and/or the final pH (i.e $pH_2$). The pH of the suspension following the addition of hydrazine is defined as $pH_2$. The effect of varying the amount of hydrazine on the crystal structure of the FeOOH precipitated from ferric nitrate is illustrated in Figure IV.9.7. The match of the XRD pattern of the samples with the ASTM standard pattern (8-98) of $\gamma$-FeOOH is very good for peak positions. However, the relative intensity of the peaks varied with the amount of hydrazine added. More interestingly, the $\gamma$-FeOOH fraction increased to a maximum level with increasing hydrazine concentration, and then with a further increase in hydrazine concentration, the relative fraction of $\gamma$-FeOOH decreased. However, for these experimental conditions, nearly pure $\gamma$-FeOOH phase was observed even at the higher hydrazine concentrations.

Several modifiers with a chemical structure similar to hydrazine, such as pyridine, ethylpyridine, and hydrazine carboxylate, were employed in an attempt to transform the ferrihydrite into crystalline FeOOH. The results indicate that none of these compounds were effective in transforming the amorphous ferrihydrite into crystalline FeOOH (Figure IV.9.8). The data in Tables IV.9.5 and IV.9.6 summarize the results of the relative

intensities ($I/I_o$) of various XRD peaks from ASTM standard, the relative areas of samples prepared from ferric chloride and ferric nitrate solutions. The area of XRD peaks from different planes (Figures IV.9.9 and IV.9.10) corresponding to $\alpha$ and $\gamma$-FeOOH phases show a variation with the amount of hydrazine, the iron salt and the chemical modifier. Thus, the ultimate crystal structure is very much dependent on the experimental variables. The total XRD peak area (Figure IV.9.11), which is the sum of the area of each XRD peak, is essentially constant and independent on the amount of hydrazine added. The fraction of $\gamma$-FeOOH increases to a maximum as the amount of added hydrazine increases, and then decrease with a further increase of hydrazine concentration (Figures IV.9.12 and IV.9.13). On the other hand, the fraction of $\alpha$-FeOOH increases linearly with the amount of hydrazine added. The results show that a [Fe]/[hydrazine] mole ratio in the range of 6 to 12 is most favorable for the transformation of ferrihydrite to $\gamma$-FeOOH.

It is well known that amorphous Fe(III) hydroxide (ferrihydrite) is formed when ferric salts are treated with alkali. Upon aging the amorphous iron(III) hydroxide transforms to a thermodynamically more stable $\alpha$-FeOOH. According to Van der Woude et. al. (IV.9.9) the phase transformation is pH dependent and transformation is extremely slow in the pH range of 4<pH>9. They suggested that the rate of transformation can be accelerated in more acid or basic environment. They also mentioned that the rate of transformation in a highly basic media is much faster than in an acidic environment. The stoichiometric equations were represented by the following equations.

$$Fe(OH)_3 + H^+(aq) \xrightarrow{Acid} Fe(OH)_2^+(s) + H_2O \rightarrow FeOOH + H_2O + H^+ \qquad \text{[IV.9.1.]}$$

$$Fe(OH)_3 + OH^-(aq) \xrightarrow{Base} Fe(OH)_2O^-(s) + H_2O \rightarrow FeOOH + H_2O + OH^- \qquad \text{[IV.9.2.]}$$

The transformation is slowed down considerably at high ionic strength (IV.9.10) and in the presence of a strongly adsorbing species such as citrate (IV.9.11,IV.9.12). According to Schertmann and Murad (IV.9.13) the transformation to goethite is a dissolution/reprecipitation process in which the nucleation rate is governed by the rate of dissolution of ferrihydrite or nucleation/crystal growth of goethite. Formation of goethite is favored by raising or lowering the pH away from the PZC of ferrihydrite (~7-8), because this promotes dissolution of ferrihydrite. Recently Cornell (IV.9.14) reported the influence of various ions and molecules on the transformation of ferrihydrite to goethite and /or haematite. According to Cornell (IV.9.14) the soluble ions can interfere in the transformation at a number of points. And also adsorbing ligands may prevent or retard the dissolution of ferrihydrite thus reducing the supply of soluble ferric species that are required for nucleation of goethite. The ability of any ligand to stabilize ferrihydrite depends on both the pH of the system and on the nature of the ligand. The extent of adsorption is related to the acid/base properties of the ligand, stereochemistry of the ligand and on the number of potential coordinating groups.

Since the transformation of amorphous iron(III) hydroxide to crystalline FeOOH is promoted in basic media; hence the formation of crystalline FeOOH in the presence of hydrazine can be explained by the following equations.

$$Fe(OH)_3 + NH_2NH_2 \rightarrow [Fe(OH)_3 \cdots\cdots NH_2NH_2] \rightarrow 2FeOOH + 2NH_4OH + 1/2\ O_2 \qquad \text{[IV.9.3.]}$$

In other words, when hydrazine is added to ferric hydroxide precipitate it may form a complex with Fe(III) hydroxide then during washing and drying the ligand i.e $NH_2NH_2$ decomposes liberating ammonia gas, which might cause an increase in pH of the precipitate, the increase in pH will accelerate the transformation of amorphous iron(III) hydroxide to crystalline FeOOH. The second possible explanation could be hydrazine may reduce part of the precipitated iron(III) to iron(II) in the first step. The transformation of the brown color $Fe(OH)_3$ precipitate to dark brown after adding hydrazine monohydrate may be because of reduction of Fe(III) to Fe(II). During aerial drying the dark color of the precipitate changes to orange yellow/yellow. The crucial steps in the process may be the formation of complex between iron and hydrazine and also reduction of part of iron(III) to iron(II). Recently Cornell and Schneider (IV.9.15) reported the formation of $\alpha$-FeOOH starting from iron(III) and L-cysteine. The method involves conversion of amorphous iron(III) hydroxide to a mixed-valence, crystalline compound by interaction with L-cysteine followed by oxidation of the intermediate phase to $\alpha$-FeOOH. A crucial step in their process was the formation of the mixed-valence precursor, and to achieve this a cysteine:Fe ratio >1.0 was required.

According to Cornell (IV.9.14) the stability of initially formed ferrihydrite depends on the nature of ligand, anions present, and solution pH. Cornell's study (IV.9.14) also points out that the adsorbing ligands may prevent or retard the dissolution of ferrihydrite. And most of the researchers (IV.9.13,IV.9.14) believe that the dissolution of ferrihydrite is one of the key factor during the formation of $\alpha$-FeOOH starting from ferrihydrite. It has

been reported (IV.9.16,IV.9.17) that the presence of small amounts of EDTA favor the formation of $\gamma$-FeOOH during the oxidation of Fe(OH)2 aqueous solutions. According to Barton et al. (IV.9.16,IV.9.17) the proportion of $\gamma$-FeOOH formed was dependent on the concentration of EDTA and oxidation temperature. These authors report that the time of addition of EDTA to the reaction mixture also affected the phase of FeOOH produced. Barton et al. (IV.9.16,IV.9.17) study on the synthesis of $\gamma$-FeOOH starting from ferrous solutions, show that the addition of EDTA improve the formation of $\gamma$-FeOOH. There are several studies on the influences of amines on the formation of $\gamma$-FeOOH. Baudisch and Albrecht (IV.9.18) reported that nitrogen-containing compounds such as pyridine and azide are effective for the formation of $\gamma$-FeOOH from an $FeCl_2$ solution. Simon et al (IV.9.19) studied in detail the influence of pyridine on the formation of $\gamma$-FeOOH from an $FeSO_4$ solution to find that pyridine interferes with the crystallization of $\gamma$-FeOOH. Recently Ishikawa et al (IV.9.20) reported the formation of $\gamma$-FeOOH from $FeSO_4$ solution in the presence of amines with pKa values higher than 8.00. These authors also observed the formation of $\alpha$ and $\gamma$-FeOOH if the pKa value of the amine is less than 7.00. Their XRD studies show that the samples prepared in the presence of amines with pKa >10.53 indicated the preferential growth of (020) plane compared to other planes. The addition of hydrazine to the ferrihydrite precipitate we caused a preferential growth of the (020), (110), (200) and (151) planes compared to other planes of $\gamma$-FeOOH phase. Similarly, the growth of the (110), (130) and (151) planes of $\alpha$-FeOOH phase also observed. The areas under these peaks varied (Figures IV.9.9 and IV.9.10) with the amount of hydrazine added. The $2\theta$ values corresponding to $\gamma$-FeOOH phase are 14.1,

27.1, 47.0 and 53.0 degrees, respectively. Similarly, the $2\theta$ values corresponding to $\alpha$-FeOOH are 21.2, 33.3 and 59.0, respectively.

In the present study we have observed that when ferric hydroxide (precipitated from ferric salt solutions) treated with hydrazine, $\gamma$-FeOOH was produced under specific reaction conditions of pH, and type of anion. We also observed that chloride ion favors the formation of $\gamma$-FeOOH while sulfate ions favor the formation of $\alpha$-FeOOH and nitrate forms both $\alpha$ and $\gamma$-FeOOH. Although the role of hydrazine is still unclear, we believe either the formation of iron-hydrazine intermediate complex /or adsorption of hydrazine on ferrihydrite followed by its decomposition/or desorption to crystalline FeOOH. The formation of $\gamma$-FeOOH in presence of chloride ions, $\alpha$-FeOOH in presence of sulphate ions (IV.9.21) and a mixture of $\alpha$ and $\gamma$-FeOOH in the presence of nitrate also suggests the preferential adsorption or coordination of hydrazine with the ferrihydrite. Several other compounds such as phenyl hydrazine, hydrazine carboxylate, pyridine etc., have been tested to make crystalline FeOOH. But none of the tested compounds produced either $\gamma$-FeOOH or $\alpha$-FeOOH.

## IV.9.5. CONCLUSIONS

In the present study we report a single step synthesis of purely crystalline $\gamma$-FeOOH starting from ferric salt solutions and hydrazine. And this is a first example of making $\gamma$-FeOOH starting from ferric iron aqueous solutions. We report the synthesis of crystalline FeOOH at low pH values and no aging is required to convert ferrihydrite to crystalline FeOOH. The presence of hydrazine and chloride ions strongly influences the transformation of ferrihydrite to crystalline $\gamma$-FeOOH. However, the formation of other crystalline FeOOH phases is mostly governed by the counter ions present in the

suspension. When there is no hydrazine the final product is X-ray amorphous in the pH range of 5 to 10.

Although there is no experimental evidence, we believe the formation of either hydrazine-ferrihydrite complex or adsorption of hydrazine on ferrihydrite prior to the transformation of ferrihydrite to crystalline FeOOH.

## IV.9.6. REFERENCES


IV.9.1. J. Dousma and P. L. de Bruyn, *J. Colloid and Int. Sci.*, **56**, 527 (1976).

IV.9.2. J. Dousma and P. L. de Bruyn, *J. Colloid and Int. Sci.*, **64**, 154 (1978).

IV.9.3. J. Dousma and P. L. de Bruyn, *J. Colloid and Int. Sci.*, **72**, 314 (1979).

IV.9.4. E. Matijevic and G. E. Janauer, *J. Colloid and Int. Sci.*, **21**, 197 (1966).

IV.9.5. C. M. Flynn, *Chem. Rev.*, **84**, 31 (1984).

IV.9.6. J. D. Bernal, D. R. Dasgupta and A. L. Mackay, *Clay Minerals Bulletin*, **21**, 15 (1959).

IV.9.7. S. Brunauer, P. H. Emmett and E. Teller, *J. Am. Chem. Soc.*, **60**, 309 (1938).

IV.9.8. J. C. P. Broekhoff and J. H. deBoer, *J. Catal.*, **9**, 15 (1967).

IV.9.9. J. H. A. Van der Woude, P. Verhees and P. L. de Bruyn, *Colloids and Surfaces*, **8**, 79 (1983).

IV.9.10. J. H. A Van der Woude and P. L. de Bruyn, *Colloids and Surfaces*, **8**, 55 (1983).

IV.9.11. U. Schwertmann, W. R. Fischer, H. Papendrof, *Trans 9th Intern. Congr. Soil. Sci.*, 1968, p645.

IV.9.12. J. H. A. Van der Woude, doctoral Thesis, Utrcht, 1983.

IV.9.13. U. Schwertmann, and E. Murad, *Clays Clay min.*, **31**, 277 (1983).

IV.9.14. R. M. Cornell, Z. Pflanzenernahr, *Bodenk*, **150**, 304 (1987).

IV.9.15. R. M. Cornell and W. Schneider, *J. Chem. Soc. Faraday Trans.*, **87**, 869 (1991).

IV.9.16. T. F. Barton, T. Price, and J. G. Dillard, *J. Colloid and Int. Sci.*, **138**, 122 (1990).

IV.9.17. T. F. Barton, T. Price, and J. G. Dillard, *J. Colloid and Int. Sci.*, **141**, 553 (1991).

IV.9.18. O. Baudisch and W. H. Albrecht, *J. Am. Chem. Soc.*, **54**, 943 (1932).

IV.9.19. A. Simon, H. H. Emons and W. D. Adam, *J. Prakt. Chem.*, **13**, 177 (1961).

IV.9.20. T. Ishikawa, H. Nishimori, A. Yasukawa, and K. Kandori, *J. Mat. Sci. Lett.*, **12**, 1359 (1993).

IV.9.21. S. Chokkaram, and B. H. Davis, unpublished results.

Table IV.9.1

Effect of pH and Hydrazine on the Crystal Structure, BET Surface Area, and Pore Volume of the Precipitate Prepared from Ferric Chloride Solutions (500 mL, 0.5M)

| Sample No. | $pH_1$* | $pH_2$** | Chemical Modifier and Concentration, M | XRD Phases | Crystallite Sizes, A | BET Surface Area, $m^2/g$ |
|---|---|---|---|---|---|---|
| 1 | 9.93 | --- | None | Amorphous | < 20 | 41.7 (0.043)# |
| 2 | 9.13 | --- | None | Amorphous | < 20 | 183.4 (0.191)# |
| 3 | 8.99 | --- | None | Amorphous | < 20 | 170.6 (0.228)# |
| 4 | 6.30 | --- | None | Amorphous | < 20 | 222.0 (0.204)# |
| 5 | 5.10 | --- | None | Amorphous | < 20 | 35.9 (0.092)# |
| 6 | 9.32 | 9.79 | $NH_2NH_2$ 0.0618 | $\alpha$-FeOOH | 352.6 359.7 | 61.2 (0.148)# |
| 7 | 6.87 | 8.26 | $NH_2NH_2$ 0.0618 | $\gamma$-FeOOH and $\alpha$-FeOOH | 282.4 190.0 | 56.5 (0.186)# |
| 8 | 6.30 | 8.15 | $NH_2NH_2$ 0.0618 | $\gamma$-FeOOH | 205.3 242.7 | 120.7 (0.203)# |
| 9 | 5.13 | 7.79 | $NH_2NH_2$ 0.0618 | $\gamma$-FeOOH | 301.2 384.1 | --- |

* $pH_1$ is the pH of iron(III) suspension after precipitation with aqueous NaOH.
** $pH_2$ is the pH of iron suspension after the addition of aqueous NaOH and hydrazine.
# Pore volume cc/g.

Table IV.9.2

Effect of pH and Hydrazine on the Crystal Structure, BET Surface Area, and Pore Volume of the Precipitate Prepared from Ferric Chloride Solutions at a pH of 6.3 (500 mL, 0.5M)

| Sample No. | $pH_2$** | Chemical Modifier Concentration, M | XRD Phases | Crystallite Sizes, A | BET Surface Area, $m^2/g$ |
|---|---|---|---|---|---|
| 10 | 8.15 | 0.0619 | $\alpha$ and $\gamma$-FeOOH | 240.1<br>251.2 | 128.9<br>(0.242)# |
| 11 | 7.82 | 0.0412 | $\gamma$-FeOOH<br>Traces of $\alpha$-FeOOH | 238.7<br>210.9 | 68.5<br>(0.182)# |
| 12 | 7.44 | 0.0206 | $\gamma$-FeOOH<br>Traces of $\alpha$-FeOOH | 282.3<br>329.4 | --- |
| 13 | 6.91 | 0.0103 | $\gamma$-FeOOH<br>Traces of $\alpha$-FeOOH | 250.9<br>329.3 | 70.5<br>(0.145)# |
| 14 | 6.60 | 0.0052 | Amorphous | < 20 | 125.8<br>(0.244)# |

** $pH_2$ is the pH of iron suspension after the addition of aqueous NaOH and hydrazine.
# Pore volume cc/g.

Table IV.9.3

Effect of pH and Hydrazine on the Crystal Structure, BET Surface Area, and Pore Volume of the Precipitate Prepared from Ferric Nitrate Solutions (500 mL, 0.5M)

| Sample No. | $pH_1$* | $pH_2$** | Chemical Modifier and Concentration, M | XRD Phases | Crystallite Sizes, A | BET Surface Area, $m^2/g$ |
|---|---|---|---|---|---|---|
| 15 | 9.13 | --- | None | Amorphous | < 20 | 48 (0.047)# |
| 16 | 8.23 | --- | None | Amorphous | < 20 | 135.6 (0.118)# |
| 17 | 7.01 | --- | None | Amorphous | < 20 | 125.8 (0.244)# |
| 18 | 5.90 | --- | None | Amorphous | < 20 | 105.9 (0.244)# |
| 19 | 5.00 | --- | None | Amorphous | < 20 | 37.9 (0.046)# |
| 20 | 8.97 | 9.42 | Hydrazine 0.0618 | $\alpha$-FeOOH | 234.1 292.6 | 113.3 (0.294)# |
| 21 | 7.96 | 8.33 | Hydrazine 0.0618 | $\gamma$-FeOOH and $\alpha$-FeOOH | 260.1 334.4 | 128.4 (0.275)# |
| 22 | 7.00 | 8.27 | Hydrazine 0.0618 | $\gamma$-FeOOH | 225.8 235.9 | 85.9 (0.269)# |
| 23 | 6.30 | 7.59 | Hydrazine 0.0618 | $\gamma$-FeOOH | 225.8 214.4 | 75.7 (0.131)# |
| 24 | 5.30 | 7.32 | Hydrazine 0.0618 | $\gamma$-FeOOH | 225.8 147.5 | 141.6 (0.216)# |

* $pH_1$ is the pH of iron(III) suspension after precipitation with aqueous NaOH.
** $pH_2$ is the pH of iron suspension after the addition of aqueous NaOH and hydrazine.
# Pore volume cc/g.

Table IV.9.4

Effect of pH and Hydrazine on the Crystal Structure, BET Surface Area, and Pore Volume of the Precipitate Prepared from Ferric Chloride Solutions at a pH of 6.3 (500 mL, 0.5M)

| Sample No. | $pH_2$** | Chemical Modifier Concentration, M | XRD Phases | Crystallite Sizes, A | BET Surface Area, $m^2/g$ |
|---|---|---|---|---|---|
| 25 | 8.26 | 0.0618 | $\alpha$ and $\gamma$-FeOOH | 275.4<br>354.6 | 89.8<br>(0.211)# |
| 26 | 7.94 | 0.0412 | $\gamma$-FeOOH<br>Traces of $\alpha$-FeOOH | 292.6<br>325.1 | 59.2<br>(0.219)# |
| 27 | 7.44 | 0.0206 | $\gamma$-FeOOH | 266.0<br>360.1 | 69.0<br>(0.138)# |
| 28 | 7.01 | 0.0103 | $\gamma$-FeOOH | 260.1<br>320.7 | 99.3<br>(0.218)# |
| 29 | 6.69 | 0.0052 | Amorphous | < 20 | 210.1<br>(0.187)# |

** $pH_2$ is the pH of iron suspension after the addition of aqueous NaOH and hydrazine.
# Pore volume cc/g.

Table IV.9.5

Relative Intensities ($I/I_o$)* Values for Various Samples, Including the ASTM Standard and the Samples Prepared from Ferric Chloride Source

| $2\theta$ Values, Degrees | ASTM Standard, Relative Intensity (Crystal Plane) | Standard (Experimental) | Sample #10 | Sample #11 | Sample #12 | Sample #13 |
|---|---|---|---|---|---|---|
| 14.1 | 100, (020) | 100 | 85 | 90 | 100 | 95 |
| 27.1 | 90, (110) | 89.4 | 100 | 95 | 99 | 100 |
| 47.0 | 70, (200) | 86.5 | 99 | 100 | 98 | 97 |
| 53.0 | 40, (151) | 36.8 | 45 | 42 | 54 | 50 |

* Where I is the intensity of an XRD peak, $I_o$ is the intensity of strongest XRD peak from that sample. $I/I_o$ = [Area of XRD peak (xi) from a sample] *100/[Area of the strongest peak from the same sample.

Table IV.9.6

Relative Intensities ($I/I_o$)* Values for Various Samples, Including the ASTM Standard and the Samples Prepared from Ferric Nitrate Source

| $2\theta$ Values, Degrees | ASTM Standard, Relative Intensity (Crystal Plane) | Standard (Experimental) | Sample #25 | Sample #26 | Sample #27 | Sample #28 |
|---|---|---|---|---|---|---|
| 14.1 | 100, (020) | 100 | 100 | 94 | 82 | 91 |
| 27.1 | 90, (110) | 89 | 87 | 85 | 100 | 96 |
| 47.0 | 70, (200) | 87 | 96 | 100 | 85 | 100 |
| 53.0 | 40, (151) | 37 | 52 | 49 | 49 | 51 |

* Where I is the intensity of an XRD peak, $I_o$ is the intensity of strongest XRD peak from that sample. $I/I_o$ = [Area of XRD peak (xi) from a sample] *100/[Area of the strongest peak from the same sample.

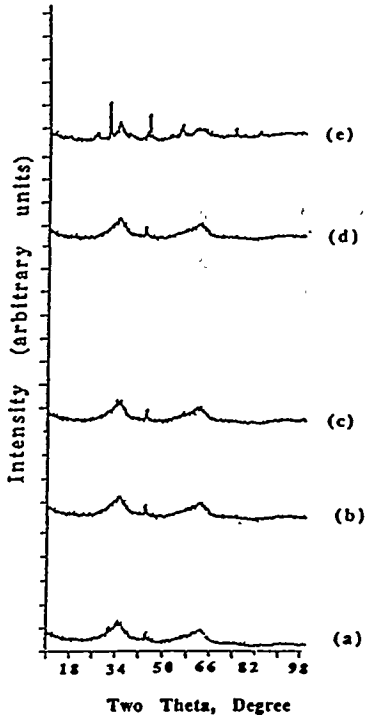


Figure IV.9.1. Effect of precipitation pH on the crystal structure of iron hydroxide or oxyhydroxide precipitated from ferric chloride aqueous solutions. The pH values are (a) 5.10, (b) 6.30, (c) 7.08, (d) 9.13, and (e) 9.93.

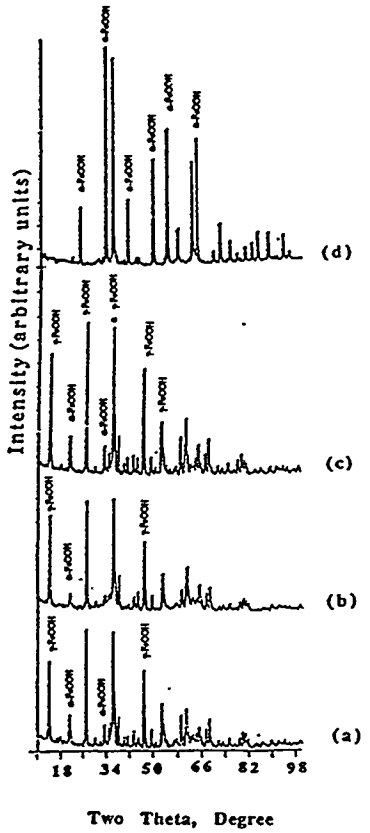


Figure IV.9.2. Effect of precipitation pH and amount of hydrazine added on the crystal structure of FeOOH precipitated from ferric chloride. The pH values ($pH_1$ and $pH_2$) of the iron suspension after precipitation with aqueous NaOH solution and after chemical treatment with hydrazine respectively are (a) 5.13, 7.79, (b) 6.30, 8.15, (c) 6.87, 8.26, and (d) 9.32, 9.79. The amount of hydrazine = 0.0618 moles.

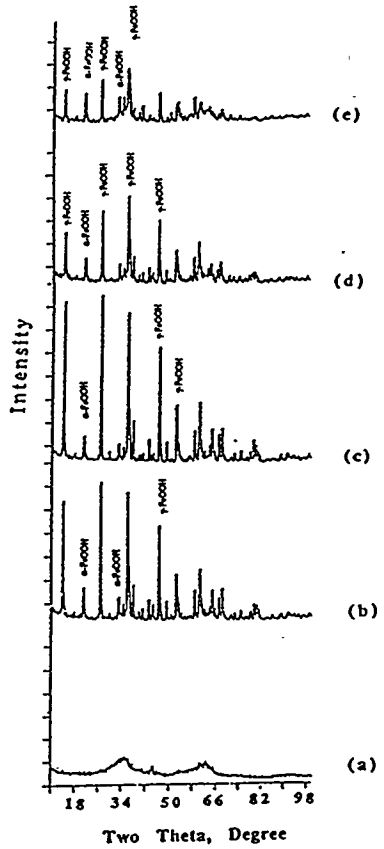


Figure IV.9.3. Effect of hydrazine on the crystal structure of FeOOH precipitated from ferric chloride. The pH values ($pH_1$ and $pH_2$) respectively are (a) 6.31, 6.60, (b) 6.28, 6.91, (c) 6.28, 7.44, (d) 6.32, 7.82, and (e) 6.32, 8.15. The Fe/hydrazine mole ratio values are (a) 48.54, (b) 24.27, (c) 12.13, (d) 6.06 and (e) 4.04.

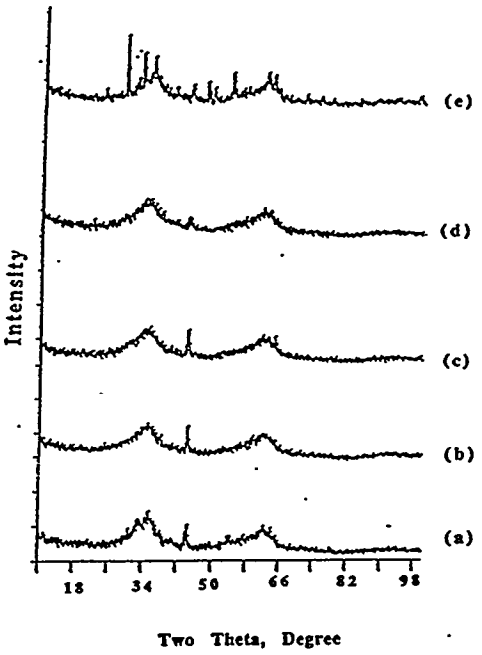


Figure IV.9.4. Effect of precipitation pH on the crystal structure of iron hydroxide or oxyhydroxide precipitated from ferric nitrate aqueous solutions. The pH values are (a) 5.00, (b) 5.90, (c) 7.01, (d) 8.23, and (e) 9.13.

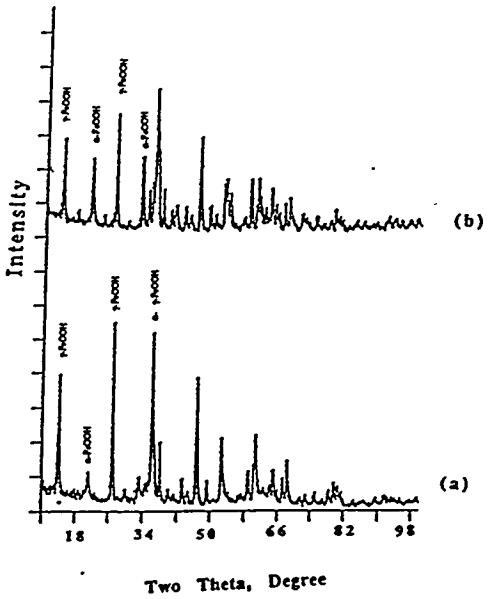


Figure IV.9.5. Effect of nitrate and hydrazine on the crystal structure of FeOOH precipitated from ferric nitrate aqueous solutions. (a) Represents chemical treatment with ammonium chloride, and (b) without ammonium chloride. The pH values ($pH_1$ and $pH_2$) are (a) 7.00, 8.27 and (b) 7.00, 7.65.

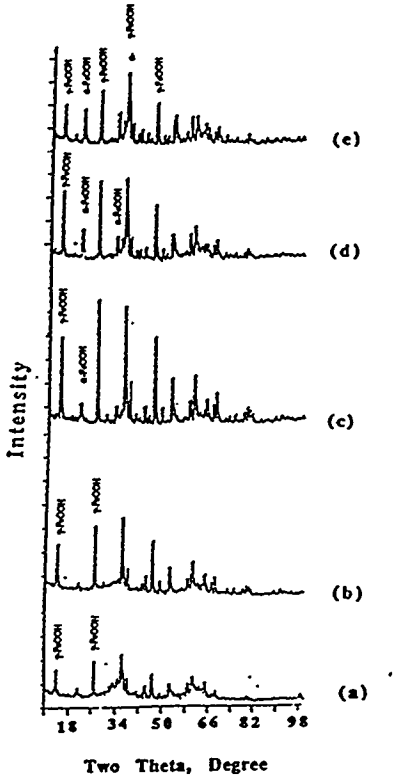


Figure IV.9.6. Effect of precipitation pH, ammonium chloride and amount of hydrazine added on the crystal structure of FeOOH precipitated from ferric nitrate. The pH values ($pH_1$ and $pH_2$) of the iron suspension after precipitation with aqueous NaOH solution and after chemical treatment with hydrazine respectively are (a) 5.30, 7.32, (b) 6.30, 7.59, (c) 7.00, 8.27, (d) 7.96, 8.33, and (d) 8.97, 9.42. The amount of hydrazine = 0.0618 moles.

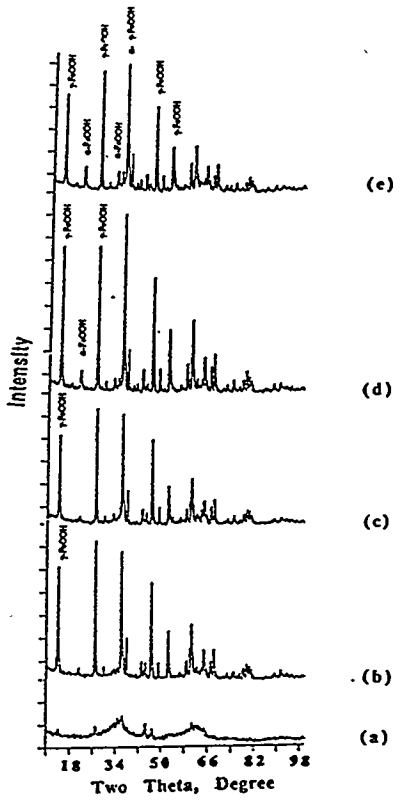


Figure IV.9.7. Effect of hydrazine and ammonium chloride on the crystal structure of FeOOH precipitated from ferric nitrate. The pH values ($pH_1$ and $pH_2$) respectively are (a) 6.31, 6.69, (b) 6.38, 7.01, (c) 6.38, 7.44, (d) 6.36, 7.94, and (e) 6.35, 8.26. The Fe/hydrazine mole ratio values are (a) 48.54, (b) 24.27, (c) 12.13, (d) 6.06 and (e) 4.04.

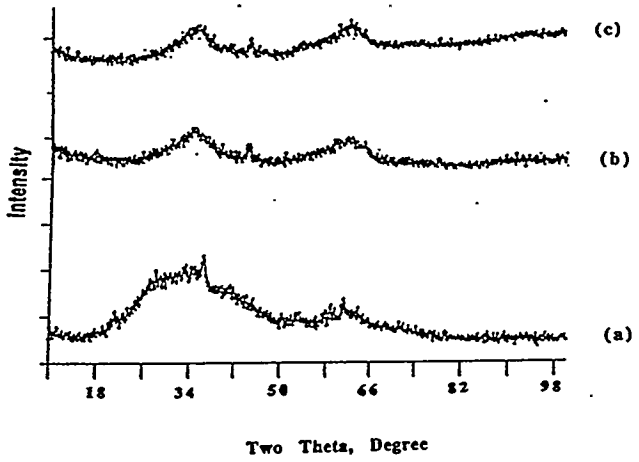


Figure IV.9.8. Effect of pyridine, ethyl pyridine and hydrazine carboxylate on the crystal structure of FeOOH precipitated from ferric chloride aqueous solutions. (a) hydrazine carboxylate, (b) ethyl pyridine, and (c) pyridine.

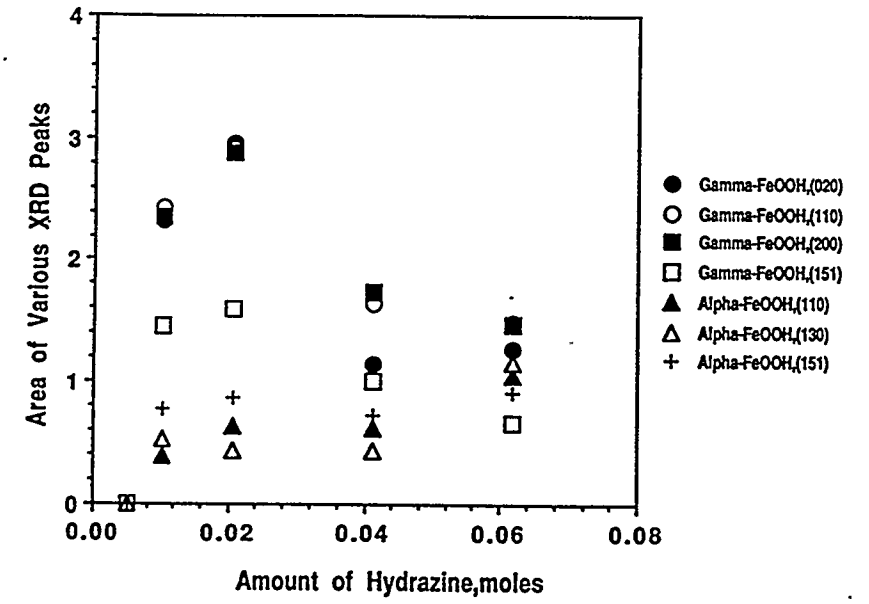


Figure IV.9.9. Effect of the amount of hydrazine on the relative XRD peak areas of $\alpha$ and $\gamma$-FeOOH phase from different planes precipitated from ferric chloride aqueous solutions.

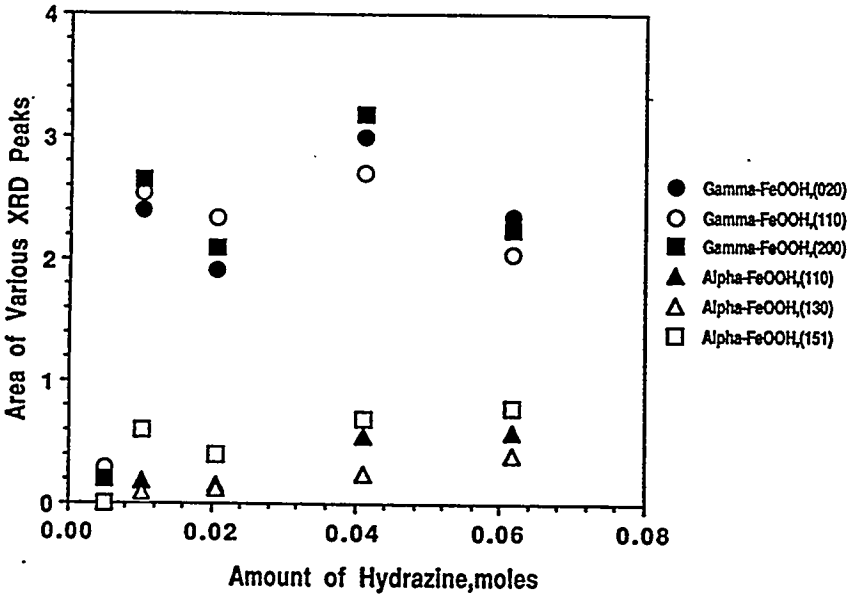


Figure IV.9.10. Effect of the amount of hydrazine on the relative XRD peak areas of $\alpha$ and $\gamma$FeOOh phases from different planes precipitated from ferric nitrate aqueous solutions.

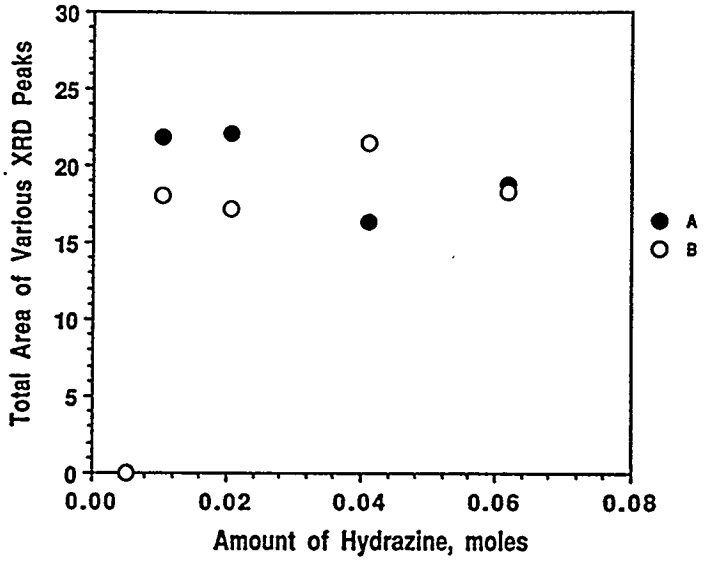


Figure IV.9.11. Effect of the amount of hydrazine on the relative total areas of XRD peaks for various samples prepared from ferric salt solutions. (●) ferric chloride system, and (○) ferric nitrate and ammonium chloride system.

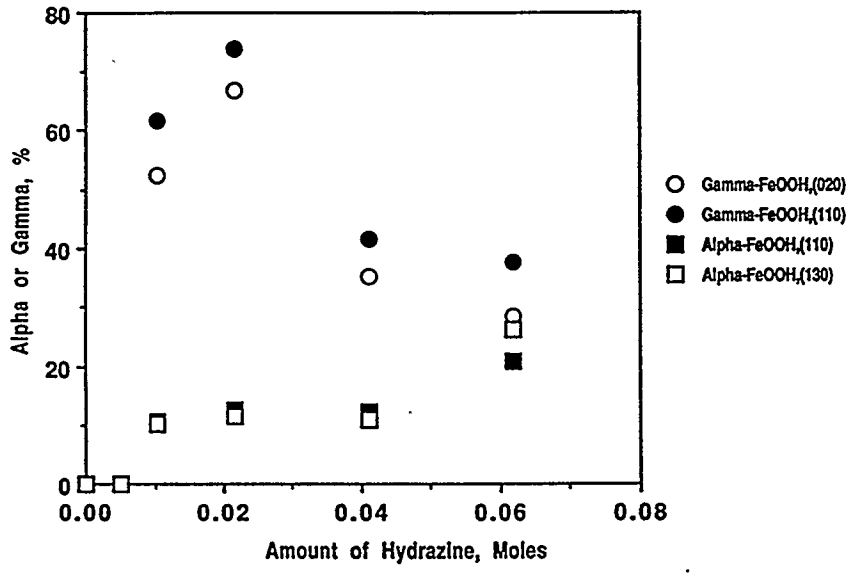


Figure IV.9.12. Effect of the amount of hydrazine on the percent of $\alpha$ and $\gamma$-FeOOH formation for the samples prepared from ferric chloride precursor.

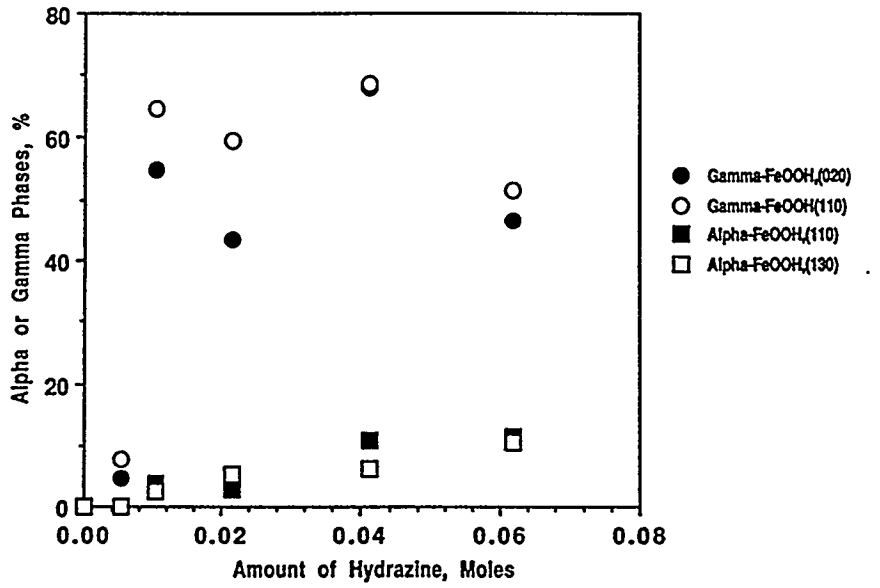


Figure IV.9.13. Effect of the amount of hydrazine on the percent of $\alpha$ and $\gamma$-FeOOH formation for the samples prepared from ferric nitrate precursor.